Liushun Wu*, Wei Gao, Dawei Xie, Liaosha Li and Yuanchi Dong

Thermodynamic Analysis of V-concentrating Phase Formation in V-bearing Steelmaking Slag Modified by MgO

Abstract: In the study, magnesium oxide acting as modifier was added to V-bearing steelmaking slag to concentrate vanadium, and then the effect of magnesium oxide on the formation of V-concentrating phase during cooling was investigated. Experimental results show that, in the case of the original slag, di-calcium silicate along with most of vanadate and phosphate in the slag forms solid solution, calcium ferrite which contains small part of vanadium in the slag and matrix without vanadium in turn precipitate during slowly cooling; For the sample with 8% MgO addition, two new phases (merwinite and V-concentrating phase) generate during slowly cooling, and the amount of di-calcium silicate decreases. Merwinite phase doesn't contain vanadium, and V-concentrating phase ($Ca_3(V,P)_2O_8{\cdot}nCa_2SiO_4$) contains 17–19% V_2O_5 by mass; For the sample with 16% MgO addition, another new phase (monticellite) precipitates from liquid slag, the phase of di-calcium silicate disappears, and most of vanadium concentrates in V-concentrating phase-$Ca_3(V,P)_2O_8{\cdot}nCa_2SiO_4$ (18–21%V_2O_5).

Keywords: V-bearing steelmaking slag, vanadium concentration, magnesium modification, V-concentrating phase

PACS® (2010). 05.70.-a

DOI 10.1515/htmp-2014-0071
Received April 28, 2014; accepted September 10, 2014;
published online November 14, 2014

1 Introduction

V-bearing magnetite distributes widely in the world, such as China, Norway, Sweden, New Zealand, Australia, the United States, India, Canada, Philippines, Poland, Chile, and Brazil. The mineral is usually used to produce steel, so a large amount of V-bearing steelmaking slag containing 2–5%V_2O_5 is produced annually. A lot of researches focused on utilization of steelmaking slag [1–5], only a few were concerned with vanadium extraction from V-bearing steelmaking slag, so there is no effective method to extract vanadium from V-bearing steelmaking slag so far. At present V-bearing steelmaking slag is usually utilized or abandoned directly without extracting vanadium. With time going, vanadium in steelmaking slag will be leached and oxidized to high valence. High valence vanadium has high toxicity, which has a great impact on environment [6–10].

In view of the above reasons, the method of selective concentrating [11, 12] was adopted to extract vanadium from V-bearing steelmaking slag in the study. Selective concentrating method has two steps, selective concentrating and selective separating. Present study just focused on the process of selective concentrating.

Since MgO is one of main components of steelmaking slag, which serving as modifier can avoid the introduction of new elements, MgO will be selected as modifier based on $CaO\text{-}SiO_2\text{-}MgO\text{-}Al_2O_3$ quaternary phase diagram [13] (The effects of silica and alumina on concentration behavior of vanadium in V-bearing steelmaking slag have been investigated in previous studies [14, 15]). The study makes it possible to recycle V-bearing steelmaking slag and reduce pollution.

2 Experimental

A high temperature furnace equipped with $MoSi_2$ heating element was used for this investigation (see Figure 1). The temperature of the furnace was controlled by a Pt – 6% Rh / Pt – 30% Rh thermocouple in an alumina tube with closed end, and the temperature of the sample was measured by another one. The variation of the temperature in the even temperature zone of the furnace was less than ±3 K.

***Corresponding author: Liushun Wu:** School of Metallurgy Engineering Anhui University of Technology, Maanshan 243032, Anhui, China. E-mail: wuliushun567@gmail.com
Wei Gao, Dawei Xie, Liaosha Li, Yuanchi Dong: School of Metallurgy Engineering Anhui University of Technology, Maanshan 243032, Anhui, China

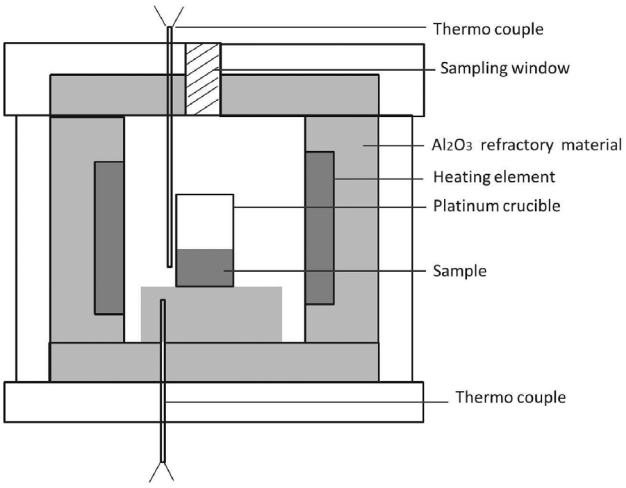

Fig. 1: Experimental set-up

The slag from Ma Steel Co. Ltd. in China (referred to as the original slag below) was adopted (which ensure practical applicability of the study). The original slag was ground into powder in a ball mill. A small amount of powder was used to determine chemical composition by XRF and titration ($FeCl_3$ solution was adopted to leach metallic iron, and then leach solution and residual were separated by filtration. The leach solution was used to determine the content of metallic iron in the original slag. The residual was dissolved by hydrochloric acid solution. The dissolved solution was used to analyze the content of FeO and Fe_2O_3.). Table 1 shows the chemical composition of the original slag. MgO (reagent grade chemical) was used in this study, and it was calcined at 1273 K for 12 hours in a muffle furnace.

In a general run, a predetermined amount of slag powder was mixed completely with a predetermined amount of magnesium oxide to obtain mixture (Table 2 shows the ratio of the original slag to magnesium oxide in the mixtures.). The mixture in platinum crucible in the high temperature furnace (see Figure 1) was heated to 1873 K at the rate of 5 K/min to melt completely, and then cooled to 1473 K at the rate of 2 K/min, keeping the temperature for 240 minutes, taking the crucible out of the furnace to quench (after removing the cover of the furnace). Besides, the law of phase precipitation was determined by equilibrium calculation and sampling using quartz tube.

Table 2: The ratio of original slag to MgO (mass%)

Sample number	Ratio (mass%)	
	Slag	MgO
1	100	0
2	92	8
3	84	16

Quenched samples were smoothed and polished for phase analysis. The phases in samples were observed by scanning electron microscopy (Cambbridge S250-M2 SEM). The compositions of phases were analyzed by energy disperse spectroscopy (Link860 EDS) affiliated to SEM.

3 Results

Figure 2 shows backscattered electron image of samples, and Table 3 presents chemical compositions of the phases corresponding to Figure 2. As seen in Figure 2 and Table 3, for the original slag (sample 1), di-calcium silicate solid solution (Ca_2SiO_4·m$Ca_3(V,P)_2O_8$, which was abbreviated as C_2S below), calcium ferrite and matrix phase precipitate during slowly cooling. Di-calcium silicate phase contains most of vanadium in the original slag, calcium ferrite phase contains the rest of the vanadium in the original slag, and matrix phase does not contain vanadium. Di-calcium silicate phase has absolute predominance in the amount in the original slag, so the phase has a low vanadium concentration. Hence none of them can act as V-concentrating phase. For the sample with 8% MgO addition (sample 2), di-calcium silicate solid solution, V-concentrating phase ($Ca_3(V,P)_2O_8$·nCa_2SiO_4, which was abbreviated as CPVS below), merwinite ($MgCa_3Si_2O_8$, which was abbreviated as C_3MS_2 below), calcium ferrite and matrix phase form during slowly cooling. Merwinite doesn't contain vanadium, while V-concentrating phase has a high content of vanadium (17–19%). In the case of the sample with 16% MgO addition (sample 3), di-calcium silicate solid solution, V-concentrating phase (which

Table 1: Chemical composition of the original slag (mass%)

CaO	SiO_2	Fe_2O_3	FeO	Fe	Al_2O_3	MgO	P_2O_5	V_2O_5	MnO	TiO_2
45.02	14.68	16.79	9.64	3.58	1.66	3.65	2.04	3.25	1.88	1.39

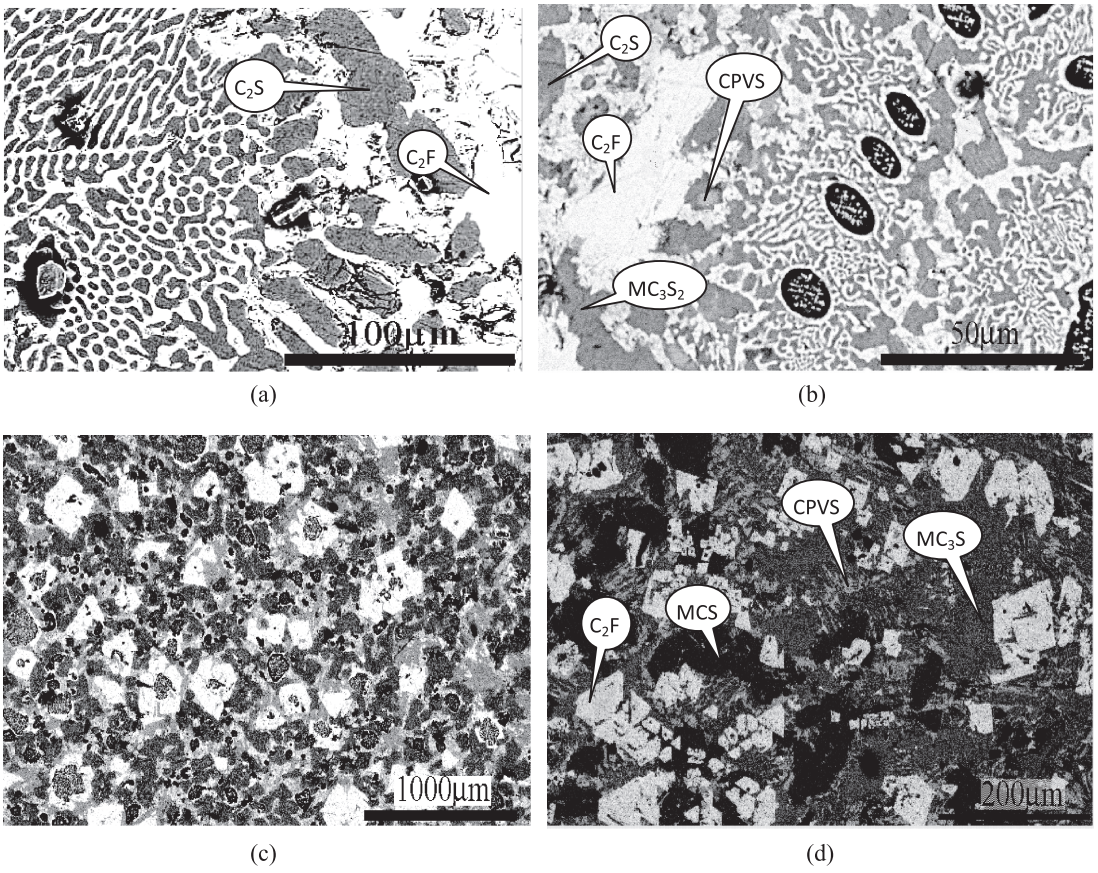

Fig. 2: SEM images of samples 1, 2 and 3. (a) The original slag, (b) the slag + 8% MgO, (c) the slag + 16% MgO (full view), and (d) the slag + 16% MgO (detail).

Table 3: Chemical composition of each phase in Fig. 1 (mole%)

No.	Phase	Mg	Al	Si	P	Ca	Ti	V	Mn	Fe
1	C_2S	1	–	23–25	0–3	65–66	–	4–7.5	–	–
	C_2F	1	0–2	6–8	–	50–52	1–3	1.5–3	8–10	21–29
	matrix	11–20	2–3	1–6	–	4–26	–	–	5–8	36–55
2	C_2S	0–2	0–2	30–32	0–2	67–68	–	1–3	–	–
	CPVS	0–2	1–2	9–12	7–10	58–60	–	17–19	–	0–2
	C_2F	0–2	0–6	0–6	–	47–50	0–2	0–1	0–2	30–35
	MC_3S_2	15–18	–	31–33	–	47–50	–	–	–	0–2
	matrix	30–32	12–14	0–4	–	4–6	3–4	0–2	0–2	30–45
3	CPVS	0–2	1–2	7–10	7–10	58–60	–	18–21	–	0–2
	C_2F	0–2	0–6	0–6	–	47–50	0–4	0–1	0–2	30–35
	MC_3S_2	17–18	–	31–33	–	47–50	–	–	–	0–2
	MCS	29–31	–	31–33	–	31–34	–	–	–	0–2
	matrix	35–40	5–6	4–5	–	8–13	1–3	–	0–2	25–30

has 18–21% vanadium concentration), merwinite, monticellite ($MgCaSiO_4$ which was abbreviated as CMS below), calcium ferrite and matrix phase precipitate during slowly cooling. Merwinite, monticellite ($MgCaSiO_4$), calcium ferrite and matrix phase hardly contains vanadium.

Comparing the samples, it is can be found that, with addition amount of MgO increasing, the yield of dicalcium silicate solid solution and the concentration of vanadium in calcium ferrite phase decrease, and the mount of V-concentrating phase increases. In brief,

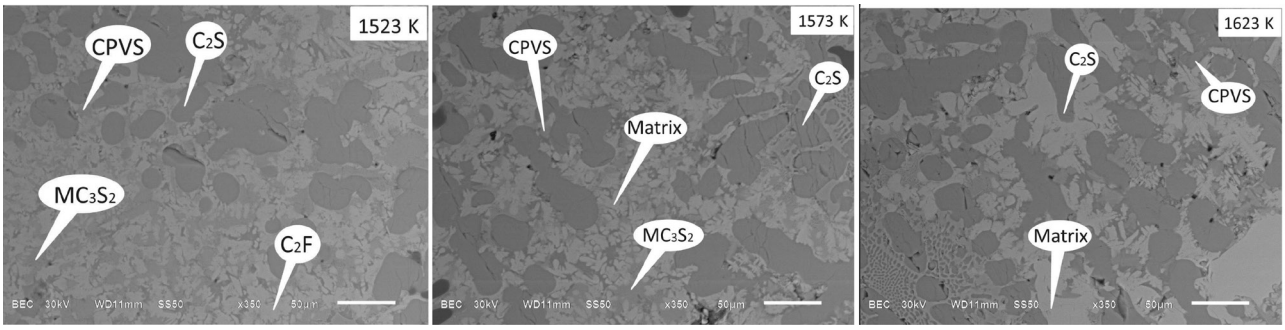

Fig. 3: SEM images for sample 2 quenched at different temperature

Table 4: Crystallization temperature of mineral phase

Phase	Temperature
Ca_2SiO_4 and $Ca_3(V,P)_2O_8$	~1623 K
Merwinite and monticellite	1623 K → 1573 K
Calcium ferrite or matrix	below 1573 K

MgO addition promotes the formation of Merwinite and monticellite, and suppresses the precipitation of di-calcium silicate solid solution, which leads to the release of vanadium in di-calcium silicate solid solution, forming V-concentrating phase.

Figure 3 presents SEM images for sample 2 which was quenched at different temperature (the chemical compositions of the phases in the images were analyzed by EDS). As shown in Figure 3, dicalcium silicate solid solution, V-concentrating phase, merwinite/monticellite, and calcium ferrite/matrix in turn precipitate during slowly cooling. Based on experimental and equilibrium calculation results, rough ranges of precipitation temperature of phases are determined, which are presented in Table 4.

4 Discussion

As known from above experimental results, calcium oxide, silica, vanadium oxide and phosphorus pentoxide in liquid slag firstly react each other to precipitate Ca_2SiO_4·$mCa_3(V,P)_2O_8$ solid solution or $Ca_3(V,P)_2O_8$·nCa_2SiO_4 solid solution which is mainly composed of calcium vanadate/phosphate during slowly cooling (As seen in Figure 4, di-calcium silicate and calcium vanadate/phosphate cannot form infinite solid solution, Ca_2SiO_4·$mCa_3(V,P)_2O_8$ solid solution is different from $Ca_3(V,P)_2O_8$·nCa_2SiO_4 solid solution. Besides, according to experimental result, $Ca_3P_2O_8$ and $Ca_3V_2O_8$ can form solid solution with any ratio. These will be described in detail in next paper). With addition

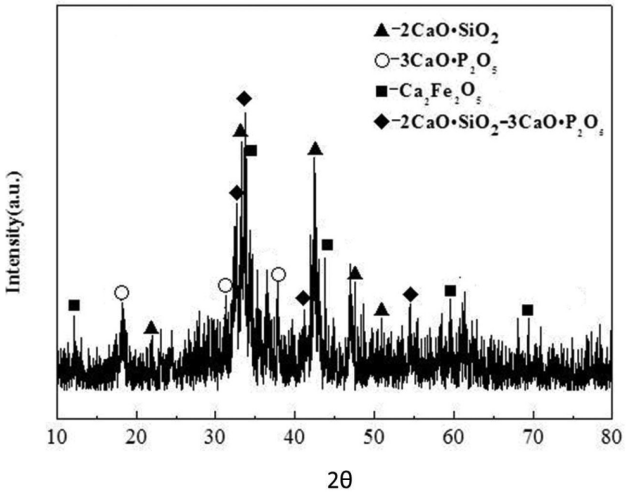

Fig. 4: XRD pattern for sample 2 quenched at 1523 K

amount of magnesium oxide increasing, the yield of Ca_2SiO_4·$mCa_3(V,P)_2O_8$ solid solution and vanadium/phosphorus concentration in it decrease, and the yield of $Ca_3(V,P)_2O_8$·nCa_2SiO_4 solid solution and vanadium/phosphorus concentration in it increase, which implies magnesium addition suppresses the formation of di-calcium silicate phase and promotes the formation of $Ca_3(V,P)_2O_8$·nCa_2SiO_4 solid solution and merwinite. The effects of MgO on the formation of Ca_2SiO_4·$mCa_3(V,P)_2O_8$ solid solution, $MgCa_3Si_2O_8$ and $MgCaSiO_4$ will be discussed using thermodynamics calculation.

4.1 The effect of MgO on the formation of di-calcium silicate

Formation reaction of Ca_2SiO_4·$mCa_3(V,P)_2O_8$ is shown in Eq. (1):

$$(2+3m-2\mu)(CaO)+(SiO_2)+(m-\mu)(V_2O_5)+\mu(Ca_2P_2O_7) \rightarrow Ca_2SiO_4\cdot mCa_3(V,P)_2O_8(S) \quad (1)$$

where

$$\Delta G_1 = \Delta G_1^0 + RT\ln\frac{a_{Ca_2SiO_4\cdot mCa_3(V,P)_2O_8}}{a_{CaO}^{2+3m-2\mu}\cdot a_{SiO_2}\cdot a_{V_2O_5}^{m-\mu}\cdot a_{Ca_2P_2O_7}^{\mu}} \quad (2)$$

$Ca_2SiO_4{\cdot}m\ Ca_3(V,P)_2O_8$ is a solid phase, so its activity is one (pure substance standard state). Based on the assumption, the following equation can be obtained.

$$\Delta G_1 = \Delta G_1^0 - (m-\mu)RT\ln(a_{CaO}^3\cdot a_{V_2O_5}) - \mu RT\ln(a_{CaO}\cdot a_{Ca_2P_2O_7}) - RT\ln(a_{CaO}^2\cdot a_{SiO_2}) \quad (3)$$

Based on experimental results, m value is about 0.15, and μ value is about 0.05. Thus, reaction (1) can be simplified as Eq. (4).

$$2.6(CaO) + (SiO_2) + 0.1(V_2O_5) + 0.05(Ca_2P_2O_7) = Ca_2SiO_4{\cdot}0.15Ca_3(V,P)_2O_8 \quad (4)$$

So, Eq. (3) can be described by Eq. (5).

$$\Delta G_2 = \Delta G_2^0 - 0.15RT\ln(a_{CaO}^4\cdot a_{V_2O_5}\cdot a_{Ca_2P_2O_7}) - RT\ln(a_{CaO}^2\cdot a_{SiO_2}) = \Delta G_2^0 - 0.15RT\ln J_1 - RT\ln J_2 \quad (5)$$

Obviously, activity product of oxides at the right of reaction Eq. (3) determines formation driving force and the yeild of $Ca_2SiO_4{\cdot}mCa_3(V,P)_2O_8$ solid solution. As shown in reaction Eq. (5), the impact of MgO on the formation of the solid solution can be attributed to MgO influencing activity product J_1 and J_2.

Figure 5 shows variation trend of activity product J_1 and J_2 with MgO addition amount (the data from thermodynamic calculation software Factsage, version: 6.2, module: Equilibrium, database: FToxid-SLAGA). As shown in Figure 5, with addition amount of MgO increasing, the curves of activity product J_1 and J_2 parallel to horizontal axis, which indicates MgO addition has a little effect on activity product J_1 and J_2. In other words, MgO addition amount within a range has no significant effect on formation driving force of di-calcium silicate and calcium vanadate/phosphate.

4.2 The effect of MgO on the formation of $MgCa_3Si_2O_8$ and $MgCaSiO_4$

Generation reaction of $MgCa_3Si_2O_8$ in liquid slag is shown in Eq. (6):

$$(MgO) + 3(CaO) + 2(SiO_2) \rightarrow MgCa_3Si_2O_8(S) \quad (6)$$

$$\Delta G_3 = \Delta G_3^0 + RT\ln\frac{a_{MgCa_3Si_2O_8}}{a_{MgO}\cdot a_{CaO}^3\cdot a_{SiO_2}^2} \quad (7)$$

Since $MgCa_3Si_2O_8$ is a solid phase, its activity is one (pure substance standard state). Eq. (7) can be expressed by Eq. (8)

$$\Delta G_3 = \Delta G_3^0 + RT\ln\frac{1}{a_{MgO}\cdot a_{CaO}^3\cdot a_{SiO_2}^2} = \Delta G_3^0 - RT\ln(a_{MgO}\cdot a_{CaO}^3\cdot a_{SiO_2}^2) = \Delta G_3^0 - RT\ln J_3 \quad (8)$$

As shown in Eq. (8), activity product J_3 directly determines formation driving force of $MgCa_3Si_2O_8$. Figure 6 shows the variation of activity product J_3 with addition amount of MgO. As seen in Figure 6, when addition amount of MgO is lower than 7 percent, activity product J_3 increases with MgO addition amount (i.e. ΔG_3 decreases

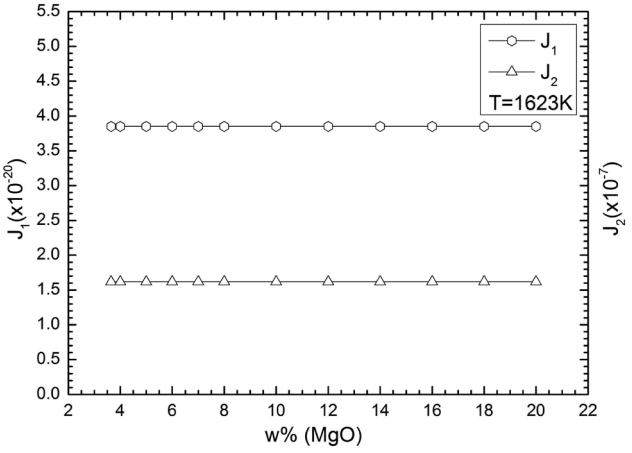

Fig. 5: The variation of activity product of J_1 and J_2 with MgO content

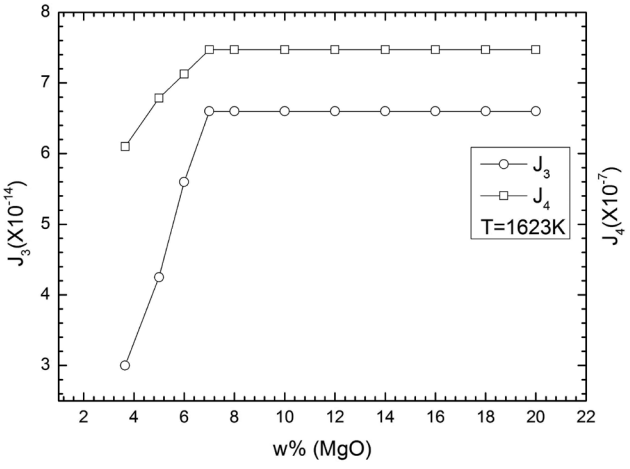

Fig. 6: The variation of activity product J_3 and J_4 with addition amount of MgO

with MgO addition amount), which indicates that MgO addition is conducive to $MgCa_3Si_2O_8$ formation. When addition amount of MgO is higher than 7 percent, activity product J_3 doesn't change with MgO addition amount, which indicates more MgO addition has no impact on formation driving force of $MgCa_3Si_2O_8$, but influences generation amount of $MgCa_3Si_2O_8$.

Generation reaction of $MgCaSiO_4$ in liquid slag is shown in Eq. (9):

$$(MgO) + (CaO) + (SiO_2) \rightarrow MgCaSiO_4(S) \tag{9}$$

$$\Delta G_4 = \Delta G_4^0 + RT \ln \frac{a_{MgCaSiO_4}}{a_{MgO} \cdot a_{CaO} \cdot a_{SiO_2}} \tag{10}$$

Since $MgCaSiO_4$ is a solid phase, its activity is one (pure substance standard state). Eq. (10) can be simplified as Eq. (11).

$$\begin{aligned} \Delta G_4 &= \Delta G_4^0 + RT \ln \frac{1}{a_{MgO} \cdot a_{CaO} \cdot a_{SiO_2}} \\ &= \Delta G_4^0 - RT \ln(a_{MgO} \cdot a_{CaO} \cdot a_{SiO_2}) = \Delta G_4^0 - RT \ln J_4 \end{aligned} \tag{11}$$

As shown in Eq. (11), activity product J_4 directly determines thermodynamics driving force of formation reaction of $MgCaSiO_4$. The variation of activity product J_4 with addition amount of MgO is shown in Figure 6. As seen in Figure 6, when addition amount of MgO is lower than 7 percent, activity product J_4 increases with addition amount of MgO, i.e. ΔG_4 decreases with addition amount of MgO, which indicates that MgO addition is conducive to $MgCaSiO_4$ formation. When addition amount of MgO is higher than 7 percent, activity product J_4 doesn't changes with addition amount of MgO, which indicates that more MgO has no effect on thermodynamics driving force of $MgCaSiO_4$ formation.

Obviously, in the sense of thermodynamic, driving forces of merwinite and monticellite formation increases with addition amount of magnesium oxide in a certain range (7%). With addition amount of MgO further increasing, driving forces of merwinite and monticellite formation almost changes no more. When addition amount of MgO reaches a certain value, driving forces of merwinite and monticellite formation predominates over that of di-calcium silicate, that is to say formation reaction of di-calcium silicate is suppressed greatly. The vanadium dissolving in dicalcium-silicate phase is released, forming high grade V-bearing phase – $Ca_3(V,P)_2O_8{\cdot}nCa_2SiO_4$.

To sum up, thermodynamic calculation shows that, when addition amount of MgO is less than 7%, the variation of addition amount of MgO has a little effect on the Gibbs free energy for formation reaction of $Ca_2SiO_4{\cdot}mCa_3(V,P)_2O_8$ phase. However, it decreases the Gibbs free energy for formation reaction of merwinite and monticellite. When addition amount of MgO is more than a certain value, thermodynamics driving force of formation reaction of merwinite and monticellite overwhelms that of di-calcium silicate, which results in a great decrease in the yield of di-calcium silicate solid solution and a great increase in the yield of merwinite and monticellite. While vanadium/phosphorus has smaller solubilities in merwinite and monticellite, which leads to the formation of a new phase-$Ca_3(V,P)_2O_8{\cdot}nCa_2SiO_4$. These have been well verified by experimental results. When addition amount of MgO is more than 7%, MgO addition has no effects on thermodynamics driving force of merwinite and monticellite formation, which is different from experimental result (the yields of merwinite and monticellite increase with addition amount of MgO). The reason is that 7% is saturation concentration for MgO for thermodynamics calculation, not for experiment.

5 Conclusions

Based on the results of experiment and thermodynamics calculation, the following conclusions can be made.

1. For the original slag, di-calcium silicate, calcium ferrite and matrix phases form during slowly cooling. Most of vanadium in the slag dissolves in di-calcium silicate phase ($Ca_2SiO_4{\cdot}mCa_3(V,P)_2O_8$), and the rest of vanadium in the slag exists in calcium ferrite phase.
2. Appropriate addition amount (8%) of MgO suppressed the precipitation of dicalcium silicate, and vanadium was released from the solid solution of $Ca_2SiO_4{\cdot}mCa_3(V,P)_2O_8$, forming V-concentrating phase $Ca_3(V,P)_2O_8{\cdot}nCa_2SiO_4$.
3. According to thermodynamics calculation, when addition amount of MgO is less than 7 percent, thermodynamics driving force of formation reaction of $MgCa_3Si_2O_8$ and $MgCaSiO_4$ increases with addition amount of MgO. When addition amount of MgO is more than 7 percent, thermodynamics driving force of formation reaction of $MgCa_3Si_2O_8$ and $MgCaSiO_4$ almost changes no more with addition amount of MgO. Beside, MgO addition amount has no effect on thermodynamics driving force of formation reaction of di-calcium silicate and calcium vanadate/phosphate.
4. The amount of V-concentrating phase and concentration degree of vanadium in the phase can be greatly promoted by controlling addition amount of MgO.

Funding: The study was supported by the National Natural Science Funds of China (no. 51174001).

References

[1] A.J. Xu, H.N. Zhang, Y. Yang, J. Cui, D.F. He and N.Y. Tian, *J. Iron and Steel Research Int.*, 19 (2012) 34–38.
[2] J.T. Gao, S.Q. Li and Y.T. Zhang et al., *J. Iron and Steel Research Int.*, 18 (2011) 32–39.
[3] N. Wang, Z.G. Liang, M. Chen and Z.S. Zou, *J. Iron and Steel Research Int.*, 18 (2011) 17–19.
[4] S. Eloneva, A. Said, C.J. Fogelholm and R. Zevenhoven, *Applied Energy*, 90 (2012) 329–334.
[5] A.S. Reddy, R.K. Pradhan and S. Chandra, *J. Mineral Processing Int.*, 79 (2006) 98–105.
[6] P. Chaurand and J. Rose, *J. Geochemical Exploration*, 88 (2006) 10–14.
[7] I.M. Madany and E. Raveendran, *Science of the Total Environment*, 116 (1992) 281–289.
[8] E. Tsiani and I.G. Fantus, *Trends Endocrinol Metab*, 8 (1997) 51–58.
[9] I. Goldwaser, D. Gefel, E. Gershonov, M. Fridkin and Y. Shechter, *J. Inorg Biochem*, 80 (2000) 21–25.
[10] A.M. Evangelou, *Critical Reviews in Oncology/Hematology*, 42 (2002) 249–265.
[11] Z.T. Sui, *Acta Metallurgica Sinica*, 33 (1997) 943–951.
[12] Z.T. Sui, *J. Chinese Rare Earth Society*, 16 (1998) 731–736.
[13] M. Allibert and H. Gaye et al., *Slag Atlas*, 2nd ed., Verlag Sthaleisen GmbH, Dusseldorf, (1995) p. 134.
[14] L.S. Li, L.S. Wu, Y.L. Su, L. Yu, X.R. Wu and Y.C. Dong, *Acta Metallurgica Sinica*, 44 (2008) 603–608.
[15] L.S. Wu, Y. Zhou and Y.C. Dong, *Applied Mechanics and Materials*, 295–298 (2013) 1729–1734.